2008 IEEE International Conference on
Robotics and Automation
Pasadena, CA, USA, May 19-23, 2008

Optimal Design and Implementation of an Energy-Efficient, Semi-Active Biped

Ting-Ying Wu and T.-J. Yeh

Abstract— **In this paper, a semi-active biped which combines the merits of both powered and passive bipeds is proposed. The semi-activeness of the biped is due to the fact that, during most of a walking cycle, only half of the joints are actuated, and the other half remain unactuated, but have passive joint springs to induce their motions. To devise a systematic design methodology for the biped, its dynamics as well as the walking constraints are carefully studied. Furthermore, an optimization procedure is proposed to compute the optimal trajectories for the actuated joints and spring constants which can lead to minimum energy consumption. The feasibility of the proposed biped is verified by hardware implementation. Experiments indicate that the semi-active biped consumes 80% less the electrical power of the powered biped that performs the same gait and is more energy-efficient than several state-of-the-art bipeds.**

I. Introduction

Depending on whether power sources are needed, bipedal walkers can be divided into two categories: powered bipeds and passive bipeds. Powered bipeds heavily rely on active control to determine when and how the external power should be activated [1]. Regardless of the fact that powered bipeds can produce dexterous motions, these systems often consume excessive power [2]. On the other hand, the passive bipeds, as proposed firstly by McGeer [3], demand neither external power nor active control. Although passive bipeds consume absolutely zero power, their stability and reliability are usually the main sources of concerns [4]. Moreover, the walking is limited on a slope.

In this research, we intend to integrate the merits of both the powered and passive bipeds by developing a semi-active biped from the viewpoint of energy and natural dynamics. The basic design and control philosophy of the proposed biped can be best understood by examining the principle of energy conservation for each walking cycle. Assuming that the biped performs stable and periodic walking on a level ground, then we have:

$$0 = W_+ - W_- - \Delta E_{lost}, \tag{1}$$

where W_+ and W_- are respectively the positive work and the negative work done by the actuators, and ΔE_{lost} denotes the energy loss due to foot-ground friction and impact. The right side of the equation equals zero because it corresponds to the change of internal energy in one cycle and should vanish by the periodicity assumption. It should be noted that most actuators used in bipeds are non-regenerative, so negative work is not recoverable. This indicates that positive work alone contributes the energy consumption of the biped. Since (1) equivalently gives $W_+ = \Delta E_{lost} + W_-$, it is clear that minimizing the energy consumption amounts to keep the energy loss and nonrecoverable negative work to minimum.

Intuitively, one can reduce the energy consumption by incorporating mechanical springs to joints of the biped. This is because that springs are a natural means of energy storage and the negative work absorbed by them is recoverable. Besides, the torques resulted from spring deformations can support the weight of the biped, so the actuator torques needed to counteract the gravity can be relieved. Another intuitive way to reduce the energy consumption is activating only part of the actuators and leaving the others unactuated. By doing so, not only is the total number of actuators performing the work reduced, but also the passive dynamics of the biped is less interfered so that it can be better exploited for energy efficiency purposes. Following this line of thought, in the proposed biped, at each joint there is a torsional spring in parallel with the actuator and the biped walks based on a semi-active control strategy, that is, only the actuators in one leg are in actuation and the actuators in the other leg are in relaxation. The rest of the paper is devoted to optimal design and implementation of this semi-active biped.

II. Dynamics for the Semi-Active Walking

The biped considered has 12 degrees of freedom and its photo and simplified schematic configuration are shown in Fig. 1. Each leg of the biped contains 6 revolute joints with two at the ankle, one at the knee, and three at the hip. At each revolute joint, there is a parallel combination of a rotary actuator and a torsional spring. Therefore, if the actuator is not powered, the corresponding joint is completely passive and the joint motion is only dictated by the spring. In the following discussion, the leg in actuation will be referred to as the active leg, and the leg in relaxation will be referred to as the passive leg.

In Fig. 2, the stick diagrams of the biped in one semi-active walking step are shown respectively in the sagittal and the frontal views. In the diagrams, the active leg is depicted by bold line segments and the passive leg by thin line segments. One walking step consists of five consecutive postures 1˜5: at posture 1, both feet of the biped are in contact with ground. However, the rear (right, passive) foot is about to be lifted off the ground that the biped is completely supported by the left

This work is supported by National Science Council in Taiwan.

Ting-Ying Wu and T.-J. Yeh are with the Department of Power Mechanical Engineering, National Tsing Hua University, Hsinchu, Taiwan 30013, R.O.C. d927706@oz.nthu.edu.tw ;tyeh@pme.nthu.edu.tw

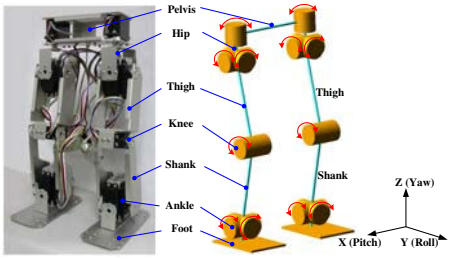

Fig. 1. The experimental semi-active biped and its 12 DOF schematic model.

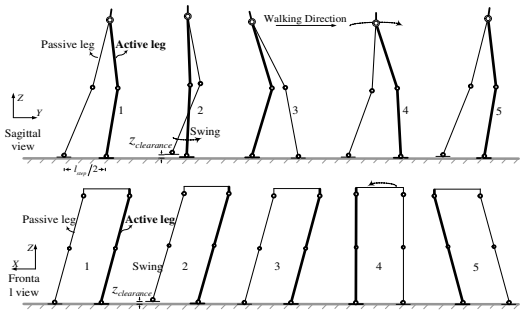

Fig. 2. The schematic figures of the semi-active walking in a step

(front, active) leg. At posture 2, the right foot has already been lifted and is swinging toward the front. At posture 3, the right foot just lands on the ground and becomes the front foot. At posture 4, the projection of pelvis is around the middle of the two feet and the front (right) leg becomes the active leg at this instant. Finally, at posture 5, the biped resumes the same posture as posture 1 except that the legs are exchanged. Let t_i denote the time instant when the i^{th} posture occurs. From t_1^+ to t_3^-, the biped is in single support phase (SSP) and from t_3 to t_5 the biped is in double support phase (DSP). Moreover, from t_1 to t_4^- the left leg is active and the right leg is passive; and from t_4 to t_5 the right leg is active and the left leg is passive.

The model for defining crucial variables for dynamic analysis is shown in Fig. 3. In these models, the symbols $\theta_{i,p}$ and $\theta_{i,r}$ are the i^{th} joint angles respectively in the pitch and roll directions. For simplification, it is assumed that the hip's yaw and roll angles are properly regulated by the controller so that the pelvis link is always perpendicular to the sagittal plane and parallel to the frontal plane. With this assumption, the dynamics in the sagittal and frontal planes becomes decoupled and the associated dynamics therefore can be derived independently.

When the foot of the active leg is assumed to be fixed to the ground, the equation of motion can be formulated in the following form:

$$\mathbf{M}(\theta)\cdot\ddot{\theta}+\mathbf{C}(\theta,\dot{\theta})\cdot\dot{\theta}+\mathbf{g}(\theta)+\mathbf{d}(\dot{\theta})+\mathbf{K}\cdot(\theta-\bar{\theta})=\tau+\mathbf{J}(\theta)^T\cdot\mathbf{f}_P. \quad (2)$$

In this equation, θ equals[1] $[\theta_{1,p}\ \theta_{2,p}\ \theta_{3,p}\ \theta_{4,p}\ \theta_{5,p}]^T$, $\mathbf{M}$ is the inertia matrix, $\mathbf{C}$ is a matrix related to the Coriolis and centrifugal effects, $\mathbf{g}$ is the gravitational torque vector, $\mathbf{d}$ is the torque vector associated joint damping, $\mathbf{K}\cdot(\theta-\bar{\theta})$ is the torque vector generated by the passive springs at the joints that $\mathbf{K}=\mathbf{diag}[k_{1,p}\ k_{2,p}\ k_{3,p}\ k_{4,p}\ k_{5,p}]^2$ and $\bar{\theta}$ is the vector corresponding to springs' relaxed angles, τ is a vector corresponding to actuation torques at the joints and due to the semi-active nature of the actuation, $\tau=[\tau_{1,p}\ \tau_{2,p}\ \tau_{3,p}\ 0\ 0]^T$, and finally $\mathbf{f}_P$ is the vector which represents the interaction force/moment between the passive foot and the ground with $\mathbf{J}(\theta)$ being the associated Jacobian matrix. It should be noted that in the formulation, to further simplify the problem, the size and the weight of the foot are assumed to be negligible, so the influence of the spring toque $k_{6,*}(\theta_{6,*}-\bar{\theta}_{6,*})$ can be lumped into the interaction force/moment vector $\mathbf{f}_P$.

By the special structure in τ, (2) can be partitioned as follows:

$$\tau_a=\mathbf{M}_a(\theta)\cdot\ddot{\theta}+\mathbf{C}_a(\theta,\dot{\theta})\cdot\dot{\theta}+\mathbf{g}_a(\theta)+\mathbf{K}_a\cdot(\theta_a-\bar{\theta}_a)+\mathbf{d}_a(\dot{\theta}_a)-\mathbf{J}_a(\theta)^T\cdot\mathbf{f}_P. \quad (3)$$

$$\mathbf{0}=\mathbf{M}_u(\theta)\cdot\ddot{\theta}+\mathbf{C}_u(\theta,\dot{\theta})\cdot\dot{\theta}+\mathbf{g}_u(\theta)+\mathbf{K}_u\cdot(\theta_u-\bar{\theta}_u)+\mathbf{d}_u(\dot{\theta}_u)-\mathbf{J}_u(\theta)^T\cdot\mathbf{f}_P. \quad (4)$$

In the two equations, the subscripts a and u respectively denote the actuated and unactuated part of the vector/matrix.

During the SSP, if the passive/unactuated leg swings without foot-ground contact, then $\mathbf{f}_P=\mathbf{0}$. Therefore, given $\mathbf{K}_u$ and $\theta_a(t)$, Runge-Kutta method can be applied to integrate (4) to numerically solve for $\theta_u(t)$. Here an operator $\mathbf{\Gamma}_{SSP}$ is used to denote the functional dependency between $\theta_u(t)$ and $\theta_a(t)$, $\mathbf{K}_u$ or

$$\theta_u(t)=\mathbf{\Gamma}_{SSP}(\theta_a(t),\mathbf{K}_u)\ . \quad (5)$$

On the other hand, during the DSP, both feet of the biped are in contact with the ground that the two legs and the ground form a closed-loop chain. By kinematic analysis, $\theta_u(t)$ can be derived as an algebraic function of $\theta_a(t)$. Denoting such an algebraic function by $\mathbf{\Gamma}_{DSP}(\theta_a(t))$, then

$$\theta_u(t)=\mathbf{\Gamma}_{DSP}(\theta_a(t))\ . \quad (6)$$

Substituting this algebraic relation into (4) and assuming that $\mathbf{J}_u(\theta)$ is nonsingular, one can directly solve for $\mathbf{f}_P$. Another operator $\mathbf{\Gamma}_{\mathbf{f}_P}$ is used to denote the functional dependency between $\mathbf{f}_P$ and $\theta_a(t)$, $\mathbf{K}_u$ or

$$\mathbf{f}_P=\mathbf{\Gamma}_{\mathbf{f}_P}(\theta_a(t),\mathbf{K}_u)\ . \quad (7)$$

Once $\theta_a(t)$, $\theta_u(t)$, and $\mathbf{f}_P$ are known and $\mathbf{K}_a$ are given, one can compute the actuation torque τ_a using (3). This, together with (5) (in SSP) or (6) and (7) (in DSP), implies that τ_a is dictated by $\theta_a(t)$ and $\mathbf{K}$, or τ_a can be succinctly written as

$$\tau_a=\mathbf{\Gamma}_{\tau_a}(\theta_a(t),\mathbf{K})\ , \quad (8)$$

where $\mathbf{\Gamma}_{\tau_a}$ is the operator denoting the functional dependency. Furthermore, by treating the biped as a system

[1]In the following, only the sagittal dynamics will be studied, but the analysis and synthesis procedures illustrated can be applied to the frontal dynamics with no difficulties.

[2]The symbol $k_{*,*}$ represents the spring constant. Its subscripts deonte which joint the spring is attached to.

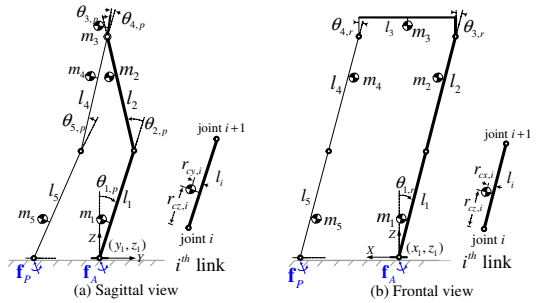

Fig. 3. Definitions of crucial variables for dynamic analysis.

of particles (with the i^{th} link modeled as a point mass m_i), assuming the knowledge of $\mathbf{f}_P(= \mathbf{0}$ for SSP, $=(7)$ for DSP), and $\theta_a(t)$, $\theta_u(t)$ (consequently the acceleration of each point mass), and then applying Newton's equations of motion to the whole biped, the interaction force/moment vector between the active foot and the ground can be solved. Again by (5) (in SSP) or (6) and (7) (in DSP), $\theta_a(t)$ and $\mathbf{K}_u$ alone determine $\mathbf{f}_A$. Denoting the functional dependency by $\mathbf{\Gamma}_{\mathbf{f}_A}$, we have

$$\mathbf{f}_A = \mathbf{\Gamma}_{\mathbf{f}_A}(\theta_a(t), \mathbf{K}_u) \tag{9}$$

III. Constraints for Achieving Stable, Periodical, Semi-active Walking

One main purpose of the paper is to devise an optimal solution for $\theta_a(t)$ and $\mathbf{K}$ so that the biped can perform stable, periodical, semi-active walking in an energy-efficient manner. To do so, constraints on the joint trajectories are investigated. Basically, there are four types of constraints.

1) Constraints for continuity: From the discussion in Fig. 2, transitions between SSP and DSP occur at postures 1, 3, 5, and control authority transfers from the left leg to the right leg at posture 4. At these four postures, the biped experiences drastic dynamic change. Regardless of the dynamic change, both the joint angles and the angular velocities should be continuous at the associated time instants. In other words,

$$\theta(t_i^-) = \theta(t_i) = \theta(t_i^+) \text{ , for } i = 1, 3, 4 \text{ and } 5 \tag{10}$$

and

$$\dot{\theta}(t_i^-) = \dot{\theta}(t_i) = \dot{\theta}(t_i^+) \text{ , for } i = 1, 3, 4 \text{ and } 5. \tag{11}$$

2) Constraints for quasi-static postures: In order for the biped to walk similar to a human being, the joint angles at postures 1, 3 and 5 are specified appropriately. The corresponding constraints are written explicitly as:

$$\theta(t_j) = \theta_d^j \text{ and } \dot{\theta}(t_j) = \mathbf{0} \text{ , for } j = 1, 3 \text{ and } 5 \tag{12}$$

where θ_d^j is the specified joint angle vector at posture j. Notice that the choice of θ_d^j's is not arbitrary but needs to meet three conditions. First of all, the actuated and unactuated parts in θ_d^j's should satisfy the algebraic equation in (6). The second condition is that $\theta_d^1 = \theta_d^5$ so as to establish the walking periodicity. Finally, the three θ_d^j's should lead to a consistent step length l_{step}.

3) Constraints for foot-ground clearance: During the entire SSP it is crucial that the swing foot should maintain a certain clearance from the ground to avoid the foot-ground interference. Such a constraint is given by

$$z_{clearance}(\theta(t)) > 0 \text{ , for } t \in \left[t_1^+ \text{ , } t_3^-\right]. \tag{13}$$

where $z_{clearance}$ denotes the clearance between the passive foot and the ground. By the configuration and the quasi-static property of posture 3, $z_{clearance}|_{t=t_3} = 0$ and the landing velocity of the swing foot also vanishes. Therefore, foot-ground impact is eliminated in this case.

4) Constraints for stability: Two more constraints need to be satisfied in order for the biped to walk in a stable manner. One is that sliding should not occur for the foot (feet) in contact with the ground. Such a constraint is relevant to $\mathbf{f}_A$ and $\mathbf{f}_P$. In the sagittal dynamics, both $\mathbf{f}_A$ and $\mathbf{f}_P$ have three components: a force in y direction, a force in z direction, and a moment in x direction. The y-force, which also acts in the tangential direction, is denoted by $(\mathbf{f}_{(\cdot)})_t$. The z-force, which also acts in the normal direction, is denoted by $(\mathbf{f}_{(\cdot)})_n$. Finally, the moment component is denoted by $(\mathbf{f}_{(\cdot)})_m$. To prevent the foot from sliding, we should have

$$|(\mathbf{f}_A)_t| \le \mu_s(\mathbf{f}_A)_n \text{ and } |(\mathbf{f}_P)_t| \le \mu_s(\mathbf{f}_P)_n \tag{14}$$

where μ_s is the coefficient of static friction.

The other stability constraint is that during walking the biped should be in dynamic equilibrium so that it does not fall down. This constraint is equivalent to limiting the total zero moment point (ZMP) associated $\mathbf{f}_A$ and $\mathbf{f}_P$ to be in the support polygon spanned by the foot (feet) contacting the ground [1]. The ZMP can be easily derived as a function of the components in $\mathbf{f}_A$ and $\mathbf{f}_P$. Take the sagittal dynamics for example, when the passive (active) foot is in front of the active (passive) foot, the ZMP is located at $\frac{(\mathbf{f}_A)_m+(\mathbf{f}_P)_m+(\mathbf{f}_P)_n \cdot l_{step}}{(\mathbf{f}_A)_n+(\mathbf{f}_P)_n}$ ($\frac{(\mathbf{f}_A)_m+(\mathbf{f}_P)_m-(\mathbf{f}_P)_n \cdot l_{step}}{(\mathbf{f}_A)_n+(\mathbf{f}_P)_n}$) with respect to the ankle of the active foot. Notice that in SSP, $\mathbf{f}_P = 0$, so the expression for ZMP location is reduced to $\frac{(\mathbf{f}_A)_m}{(\mathbf{f}_A)_n}$.

IV. An Optimization Procedure for Determining Optimal Joint Trajectories and Spring Constants

In order to minimize the control energy in one walking cycle, the following performance index

$$J = \int_{t_1}^{t_5} \|\tau_a(t)\|^2 \, dt \, . \tag{15}$$

is defined. By (8), the performance index indeed is dictated by $\theta_a(t)$ and $\mathbf{K}$. In this section, an optimization procedure is proposed to determine optimal $\theta_a(t)$ and $\mathbf{K}$ to minimize

such a performance index. Because the biped experiences drastic dynamic change at postures 1, 3, 4 and 5 in the optimization, $\theta_a(t)$ is assumed to be a concatenation of three vectorial, polynomial trajectories $\theta_{a\_SSP}(t)$, $\theta_{a\_DSP1}(t)$ and $\theta_{a\_DSP2}(t)$ respectively defined in $[t_1, t_3]$, $[t_3, t_4]$ and $[t_4, t_5]$ and parameterized as follows:

$$\begin{array}{ll} \theta_{a\_SSP}(t) = \mathbf{A}_{SSP}\mathbf{h}(t), & \text{for } t \in [t_1, t_3] \\ \theta_{a\_DSP1}(t) = \mathbf{A}_{DSP1}\mathbf{h}(t), & \text{for } t \in [t_3, t_4] \\ \theta_{a\_DSP2}(t) = \mathbf{A}_{DSP2}\mathbf{h}(t), & \text{for } t \in [t_4, t_5] \end{array} \quad (16)$$

where $\mathbf{h}(t) = [1\ t\ t^2\ \cdots\ t^m]^T$ with m being the order of polynomials, and $\mathbf{A}_{(\cdot)}$'s are matrices of suitable dimensions and contain parameters of the polynomial trajectories for the joints in the active leg. The optimization problem can now be posed as

$$\begin{aligned} \min_{A_{SSP}, A_{DSP1}, A_{DSP2}, K} \Big(& \int_{t_1}^{t_3} \left\| \mathbf{\Gamma}_{\tau_a}(\mathbf{A}_{SSP}\mathbf{h}(t), \mathbf{K}) \right\|^2 dt \\ & + \int_{t_3}^{t_4} \left\| \mathbf{\Gamma}_{\tau_a}(\mathbf{A}_{DSP1}\mathbf{h}(t), \mathbf{K}) \right\|^2 dt \\ & + \int_{t_4}^{t_5} \left\| \mathbf{\Gamma}_{\tau_a}(\mathbf{A}_{DSP2}\mathbf{h}(t), \mathbf{K}) \right\|^2 dt \Big) \end{aligned}$$

subjected to (10) ~(14) and the ZMP stability constraint, (17)

in which the constraints can be alternatively expressed in terms of $\theta_a(t)$ and $\mathbf{K}$ by (5), (6), (7) and (9).

To solve the optimization problem numerically, we discretize the interval $[t_1, t_5]$ into N equal-spaced time instants (with N sufficiently large and t_3, t_4 being two of the time instants) and approximate each of the integrals in (17) by a summation of $\left\| \mathbf{\Gamma}_{\tau_a}(\cdot, \cdot) \right\|^2$ evaluated at all the time instants at the respective interval. Furthermore, the continuous inequalities in (13), (14) and the ZMP stability constraint are also evaluated at all the time instants at the respective interval(s) to construct a set of discretized inequalities.

The discrete form of the problem is in a standard format for nonlinear, constrained optimization in MATLAB® Optimization Toolbox, so the function *fmincon* in this package [6] is used to solve the problem numerically. When the *fmincon* function is used to solve for the optimal $\mathbf{A}_{(\cdot)}$'s and $\mathbf{K}$, it is found that due to the vast numbers of parameters and constraints involved, convergence of the numerical iteration is not easy to achieve. In order to obtain a convergent solution for the relevant parameters but still maintain their optimality to certain degree, four modifications are made to the optimization problem.

First of all, it is assumed that the bounds for each of the diagonal components of $\mathbf{K}$ are given. Rather than finding $\mathbf{K}$ directly using the *fmincon* function, the solution space of $\mathbf{K}$ is divided into a grid and the optimization problem is solved repeatedly for each grid point in a brute force manner. The solution which results in the lowest performance index is adopted as the optimal one.

Secondly, the constraint associated with ZMP stability is relaxed when solving the optimization problem. Such a stability condition is examined after an optimal solution is reached. If ZMP stability does not hold, depending on which phase(s) it is violated, the respective time duration(s) ($t_1 - t_3$ for SSP, and $t_3 - t_5$ for DSP) is (are) lengthened. By lengthening the time duration(s), the speed, consequently the dynamic effect, of the biped are reduced and it is easier to make the ZMP stable.

Thirdly, instead of solving for all the three $\mathbf{A}_{(\cdot)}$ matrices simultaneously, the three integrals in (17) are minimized separately in a sequential manner. The sequential optimization is conducted in the way that $\theta_{a\_SSP}(t_3)$ $(= \mathbf{A}_{SSP}\mathbf{h}(t_3))$ and $\dot{\theta}_{a\_SSP}(t_3)$ $(= \mathbf{A}_{SSP}\dot{\mathbf{h}}(t_3))$ obtained from minimizing the first integral are substituted as initial conditions for the optimization of the second integral, and $\theta_{a\_DSP1}(t_4)$ $(= \mathbf{A}_{DSP1}\mathbf{h}(t_4))$ and $\dot{\theta}_{a\_DSP1}(t_4)$ $(= \mathbf{A}_{DSP1}\dot{\mathbf{h}}(t_4))$ obtained from minimizing the second integral are substituted as initial conditions for the optimization of the third integral. With such a modification, the set of the $\mathbf{A}_{(\cdot)}$ matrices resulted is considered to be only a suboptimal solution.

Finally, in the simulation for computing the optimal $\mathbf{A}_{SSP}$ that minimizes the first integral in (17), it is found that numerical convergence still can not be achieved. The failure in convergence is attributed to the strict constraints, particularly the foot-ground clearance constraint. To bypass the convergence issue, one observes from the kinematics of the biped that its step-size is mainly dictated by the hip joint motion. Based on this reasoning, the $\mathbf{A}_{SSP}$ matrix is decomposed as $\mathbf{A}_{SSP} = [\bar{\mathbf{A}}_{SSP}^T\ \mathbf{a}]^T$ in which the vector $\mathbf{a}$ contains parameters of the polynomial trajectories for the hip joint, and $\bar{\mathbf{A}}_{SSP}$ contains parameters for the rest of the joint. Then the optimization problem is divided into two parts. The first part assumes a given $\bar{\mathbf{A}}_{SSP}$ and computes the optimal $\mathbf{a}$ which satisfies only the posture constraint and the nonsliding constraint. The second part assumes a given $\mathbf{a}$ and computes the optimal $\bar{\mathbf{A}}_{SSP}$ which satisfies only the foot-ground clearance constraint and the nonsliding constraint. These two optimizations are cross-iterated until the 2-norm of the difference between two $\theta_{a\_SSP}(t)$'s from the two optimizations converges to within a preset tolerance (say, 10^{-5}).

The flow chart of the final optimization procedure which incorporates the four modifications is depicted in Fig. 4.

V. Simulation Results

The optimization procedure is applied to the bipedal model in Fig. 3 with parameters listed in Table I. The assumed actuated joint angles at postures 1 and 3 are listed in Table II and the postures lead to $l_{step} = 8cm$. It is also assumed that t_1=0s, t_3=0.5s, t_4=1s, t_5=1.5s, so the average speed is $\frac{l_{step}}{2(t_5 - t_1)}$=2.67$\frac{cm}{s}$. The relaxed spring angles for the ankle, knee, and hip are taken as the averages of the associated joint angles at posture 1 and 3. The viscous damping coefficient for each joint and the coefficient of static friction (μ_s) between the foot and the ground are respectively adopted[3] to be $0.488\frac{N \cdot m \cdot s}{rad}$ and 1.05.

In the optimization, the joint trajectories of the active leg are chosen as 7^{th} order polynomials. Using the flow chart in

[3]The two coefficients are obtained by performing identification experiments on the bipedal prototype presented in the next section.

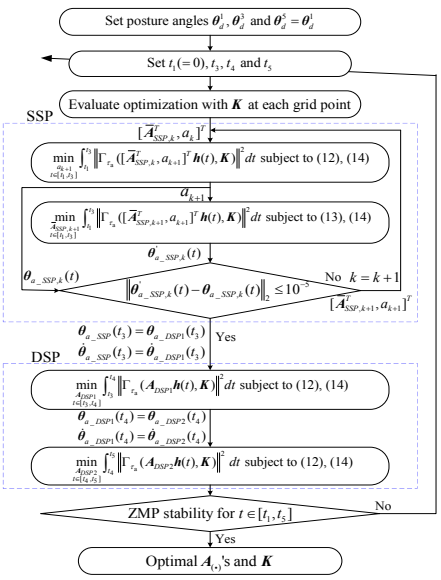

Fig. 4. The flow chart of optimization procedure

TABLE I

KINEMATIC PARAMETERS OF THE BIPEDAL MODEL

	shank ($i=1$)	thigh ($i=2$)	pelvis ($i=3$)
Length l_i (m)	0.1	0.1	0.09
Mass m_i (kg)	0.25	0.24	0.19
Center of mass $r_{cx,i}$ (m)	0	0	0.045
Center of mass $r_{cy,i}$ (m)	-0.01	-0.01	-0.01
Center of mass $r_{cz,i}$ (m)	0.01	0.085	0.025

Fig. 4, the optimal $\mathbf{A}_{(\cdot)}$'s and $\mathbf{K}$ are successfully computed. Notice that although the control energy is minimized in this case, it is under the assumption that all the springs obey linear constitutive relations. Apparently, if one relaxes this assumption or makes the springs nonlinear, the control energy can be further reduced. In this research, in addition to the original linear spring, we also consider appending another spring to the joint that one end of the spring is attached to the link, and the other end is free but is set at a designated angle. When the joint rotation is small, this appended spring is in idle state. However, when the joint rotation exceeds the designated angle, the free end is compressed by the other link and restoring torque is generated by the spring. Here the two-spring combination at each joint is referred to as the composite spring. The constitutive relationship for the composite spring at the i^{th} joint can be written in a

TABLE II

ASSIGNED CONFIGURATIONS AT POSTURES 1 AND 3

	$\theta_{1,p}$	$\theta_{2,p}$	$\theta_{3,p}$	$\theta_{1,r}$	$\theta_{3,r}$
Posture 1	$\frac{18.0}{180}\pi$	$\frac{33.1}{180}\pi$	$\frac{-20.0}{180}\pi$	$\frac{22.5}{180}\pi$	$\frac{22.5}{180}\pi$
Posture 3	$\frac{13.9}{180}\pi$	$\frac{30.8}{180}\pi$	$\frac{-0.65}{180}\pi$	$\frac{22.5}{180}\pi$	$\frac{22.5}{180}\pi$

(Unit : radian)

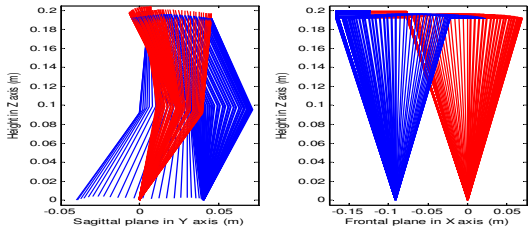

Fig. 5. The consecutive stick figures of the walking gait in sagittal and frontal views.

piecewise-linear manner:

$$\tau_i^k(\theta_{i,p}) = \begin{cases} k_{i,p} \cdot (\theta_{i,p} - \bar{\theta}_{i,p}) \ , \text{ if } \theta \le \bar{\theta}'_{i,p} \\ k_{i,p} \cdot (\theta_{i,p} - \bar{\theta}_{i,p}) + k'_{i,p} \cdot (\theta - \bar{\theta}'_{i,p}) \ , \text{ else } . \end{cases} \quad (18)$$

in which τ_i^k is the composite spring torque, $k_{i,p}$ and $k'_{i,p}$ are respectively the constants of the original linear spring and the appended spring, $\bar{\theta}_{i,p}$ is the relaxed angle of $k_{i,p}$, $\bar{\theta}'_{i,p}$ is the activation angle for $k'_{i,p}$.

The torques of the composite springs replace $\mathbf{K} \cdot (\theta - \bar{\theta})$ in (2) and the optimization is reconducted using the modified dynamic equation. The optimization assumes that $k'_{i,p}$'s and $\bar{\theta}'_{i,p}$'s are given and they are determined as follows. Because from Fig. 2 it is seen that joints of either leg are bent mostly when it is the active leg at posture 3, in order for the the appended springs to support the biped's weight without hindering the swinging motion, the free-end angles ($\bar{\theta}'_{i,p}$) are set close to the corresponding joint angles at posture 3. By doing so, the appended springs are only activated for the active leg near posture 3. As for determining the appropriate $k'_{i,p}$ value, in order for the composite springs to support the biped at posture 3, one simply sets

$$k'_{i,p} = \frac{g_{ai}(\theta(t_3)) + k_{i,p} \cdot (\theta_{i,p}(t_3) - \bar{\theta}_{i,p})}{(\bar{\theta}'_{i,p} - \theta_{i,p}(t_3))} \ , \ i = 1, 2, 3 \quad (19)$$

where $g_{ai}(\theta(t_3))$ is the i^{th} component of gravitational torque vector in (3) evaluated at $t = t_3$. Once the $k'_{i,p}$'s and $\bar{\theta}'_{i,p}$'s for one leg are determined, the corresponding values for the other leg can be obtained by symmetry.

Optimization with the assigned properties for the appended springs generates a new set of optimal $\theta_a(t)$ and $\mathbf{K}$. The corresponding stick diagrams of the walking gait in the sagittal and frontal views are plotted in Fig. 5. Notice that in the simulation of the optimal gait, the ZMP always stays in the stable polygons spanned by the supporting foot (feet) during SSP or DSP. Consequently, the biped is dynamically stable.

VI. HARDWARE IMPLEMENTATION AND EXPERIMENTAL RESULTS

In the actual biped in Fig. 1, DC motors with gear reduction are used as actuators and the mechanical links are made of light aluminum alloy. Torsional coil(s) is (are) attached to each joint to implement the linear (composite) spring design in the model. There is also a potentiometer at each joint to measure the joint angle. The reference trajectory and the

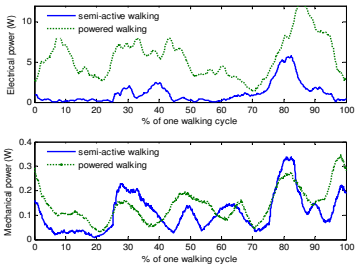

Fig. 6. The electrical and mechanical powers for the biped in the semi-active mode and the powered mode.

control algorithm (PD + feedforward) are carried out on a real-time digital signal processor (dSPACE^{TM} DS1103).

The $\theta_a(t)$ and springs' constitutive relations adopted in the experiments are similar to those obtained from optimization. In experiments, the biped walks with 1.5 seconds per step. The video demonstration of the experiment can be found in http://ldsc.pme.nthu.edu.tw/files/Robot/SABW.wmv.[4] In the experiment, instead of switching the control actuation instantly in middle of DSP as in simulation, the control gains of the active (passive) leg are changed smoothly from 100% (0%) to 0% (100%) within 1.5% of a walking cycle. By doing so, the jerky motion caused by instantaneous control authority transfer can be avoided.

A. Experimental Power Analysis

In Fig. 6, the histories of total electrical and absolute value of mechanical powers consumed in a walking cycle are recorded. For the purpose of comparing the energy efficiency of semi-active walking to powered walking, the torsional coils are removed and the biped walks in the powered mode. Although by the lower half of Fig. 6, the total mechanical powers of the two modes of walking are about the same, calculation on the upper half of the figure indicates that the powered walking mode consumes about five times the average electrical power of the semi-active mode. Such a phenomenon could be attributed to the fact that in powered walking, some motors perform much negative mechanical work. The negative electrical work associated with the negative mechanical work is not recoverable, so the total electrical power consumption is increased.

Here we also compare the energy efficiency of our semi-active biped with humans and other bipeds. To do so, a dimensionless energetic cost of transport C_{et} = (electrical energy)/(weight×traveled distance) is defined. This cost allows one to make fair comparison on the electrical energy efficiency regardless of the weights and the speeds of the walkers. Table III lists the C_{et} values for the human being, our biped, and other bipeds [5]. According to this table,

[4]A second prototype with on-board microprocessor, batteries, and interfacing circuitry is also constructed. The prototype is operated without umbilical cords, but its motion is less smooth because the on-board microcomputer has much less computing power than the digital signal processor. Its video demonstration can be found in http://ldsc.pme.nthu.edu.tw/files/Robot/SABW2.wmv.

TABLE III

THE *Cet* COMPARISION FOR THE SEMI-ACTIVE BIPED AND OTHER BIPEDS

Walking Object	C_{et}
Human	0.2
Our semi-active biped	1.81
T.U. Delft's Denise	5.3
Honda's Asimo	3.2
Cornell's powered biped	0.2

although our biped is about an order of magnitude less efficient than the human walking, it is more efficient than the bipeds except Cornell's. Particularly, it is 43% more efficient than Honda Asimo, which uses electrical motors with high conversion efficiency to perform powered walking. Clearly, it is the semi-active nature of our biped that allows it to outperform Asimo in the energy efficiency aspect. It should be noted that although Cornell's powered biped achieves the same walking efficiency as the human being, it has curved feet and only has two actuators (at the ankle) thus it could suffer stability problems. Furthermore, it also can not perform as dexterous motions as our biped which is equipped with 12 actuators.

VII. CONCLUSIONS

In this paper, a biped which combines the merits of both powered and passive bipeds is proposed. The biped is referred to as semi-active because during the walking cycle, only half of the motors are actuated. In order to fully exploit the semi-activeness for energy saving, the trajectories for the actuated joints and joints' spring constants are computed by an optimization procedure. The feasibility of the proposed biped, including the system design and the control performance, is verified by hardware implementation. Experiments indicate that the semi-active biped is indeed more energy-efficient than several state-of-the-art bipeds. On-going research is focused on incorporating more advanced control schemes to the biped so that it can learn the optimal trajectories through experiments.

REFERENCES

[1] A. Takanishi, H. Lim, M. Tsuda, and I. Kato, "Realization of Dynamic Biped Walking Stabilized by Trunk Motion on a Sagittally Uneven Surface, " *IEEE International Workshop on Intelligent Robots and Systems*, pp. 323-330, 1990.

[2] K. Hirai, M. Hirose, Y. Haikawa, and T. Takenaka, "The Development of Honda Humanoid robot," *IEEE International Conference on Robotics and Automation*, pp. 1321-1326, May 1998.

[3] T. McGeer, "Passive Dynamic Walking," *International Journal of Robotics Research*, Vol. 9(2), pp. 62-82, 1990a.

[4] S. Collins, M. Wisse, and A. Ruina, "A Three-Dimensional Passive Dynamic Walking Robot with Two Legs and Knees," *The International Journal of Robotics Research*, Vol. 20, No. 7, pp. 607-615, 2001.

[5] S.H. Collins, and A. Ruina, "A Bipedal Walking Robot with Efficient and Human-Like Gait," *in Proc., IEEE International Conference on Robotics and Automation*, pp. 1983-1988, May 2005.

[6] Optimization Toolbox User's Guide, MathWorks, Inc., Natick, Massachusetts, 1996.